Monthly Notices of the ROYAL ASTRONOMICAL SOCIETY

MNRAS **504,** 1565–1570 (2021) doi:10.1093/mnras/stab958
Advance Access publication 2021 April 9

Atomistic simulations of the free-energy landscapes of interstellar chemical reactions: the case of methyl isocyanate

Giuseppe Cassone,[1]★ Franz Saija,[1] Jiri Sponer,[2] Judit E. Sponer,[2] Antonio Jiménez-Escobar,[3] Angela Ciaravella[3] and Cesare Cecchi-Pestellini[3]★

[1]*CNR–IPCF, Viale Ferdinando Stagno d'Alcontres 37, I-98158 Messina, Italy*
[2]*Institute of Biophysics of the Czech Academy of Sciences, Královopolska 135, CZ-61265 Brno, Czech Republic*
[3]*INAF – Osservatorio Astronomico di Palermo, P.za Parlamento 1, I-90134 Palermo, Italy*

Accepted 2021 April 1. Received 2021 April 1; in original form 2021 January 29

ABSTRACT

Although complex organic molecules are observed in a wide variety of environments, chemical reaction networks heading to their formation are higly debated. It is a major endeavour to model the rates of reactions and incorporate them into chemical networks. The vast majority of the computational investigations in astrochemistry take into consideration oversimplified molecular models where chemical reactions are simulated under vacuum conditions (gas phase) and with crudely approximated entropic contributions to the free energy. We use density functional theory-based molecular dynamics techniques coupled with state-of-the-art metadynamics methods to investigate the role of ices embedding the reactants in shaping the free-energy landscape of selected reactions. Ices are chemically defined at the same level of theory of the reactants themselves. We consider as test case the transformation of methane and isocyanic acid into molecular hydrogen and methyl isocyanate, a species bearing similarities with peptide bonds. We examine the thermodynamically unfavoured case of very stable reactants to magnify modifications in the energy configuration induced by a solid amorphous water ice, either pure or mixed with CO. The presence of an active medium modifies significantly the free-energy surface, widening the path connecting reactants and products, and decreasing substantially the energy barriers. Ices not only act as gatherers of reactants, but also create thermodynamic conditions favouring chemical evolution.

Key words: astrochemistry – molecular processes – ISM: molecules.

1 INTRODUCTION

Organic molecules are observed in a wide variety of environments in the Galaxy, including gas surrounding young solar-type stars. Their presence suggests that the synthesis of such species predates the formation of planets. The production of organic material in space, in particular at the early stages of star formation, may be thus critical to tracing the evolution of simple molecular species into a potentially life-bearing chemistry.

Some of those complex organic species discovered in space (see McGuire 2018, for a detailed inventory), methyl isocyanate (CH_3NCO), isocyanic acid (HNCO), and formamide (NH_2CHO), bear a structural similarity with peptide bonds, key parts of proteins. The condensation of formamide has been shown to be a robust and widespread chemical pathway affording molecules necessary for the origin of life (e.g. Sponer et al. 2012, 2016a; Ferus et al. 2015; Saladino et al. 2015; Suárez-Marina et al. 2019). Methyl isocyanate is thought to take part in the synthesis of short amino acid chains (Pascal, Boiteau & Commeyras 2005), and to be a plausible prebiotic activating reagent (e.g. Bonfio et al. 2020). Understanding the formation of this class of molecules goes beyond the straightforward modelling of interstellar regions, as conceivably, prebiotic reaction pathways constructed in the laboratory could have occurred during the prebiotic evolution of the molecules of life.

While formamide (Rubin et al. 1971) and isocyanic acid (Snyder & Buhl 1972) were observed shortly after the detection of ammonia (Cheung et al. 1968) – the first polyatomic species discovered in space – the positive identification of methyl isocyanate occurred just few years ago (Halfen, Ilyushin & Ziurys 2015). Even more recent is the discovery of the isocyanate radical NCO by Marcelino et al. (2018).

The observations of CH_3NCO rotational emission towards Sgr B2(N) followed its tentative (and questioned; see Altwegg et al. 2017) identification in the comet 67P/Churyumov–Gerasimenko through mass spectroscopy onboard the *Rosetta* spacecraft's Philae lander (Goesmann et al. 2015). CH_3NCO has also been observed in the warm, dense inner regions of the cocoon of dust and gas surrounding the young, low-mass solar-type protostellar binary IRAS 16293−2422 (Martín-Doménech et al. 2017; Ligterink et al. 2018), and in the hot molecular core G10.47+0.03 (Gorai et al. 2020). Finally, as most other complex organic molecules, methyl isocyanate has not been yet detected in protoplanetary discs. While CO, HCO, and H_2CO are often abundant molecules in the cold zones of discs, among the species at the next level of complexity solely formic acid (HCOOH), methanol (CH_3OH), and acetonitrile (CH_3CN) have been observed, and only in a few regions (Öberg et al. 2015; Walsch et al. 2016; Carney et al. 2017; Favre et al. 2018; Podio et al. 2019).

★ E-mail: cassone@ipcf.cnr.it (GC); cesare.cecchipestellini@inaf.it (CC-P)

Both gas- and condensed-phase formation mechanisms have been applied in chemical models to explain the presence of CH_3NCO. Martín-Doménech et al. (2017) inferred that the production of methyl isocyanate might proceed in the gas phase (Halfen et al. 2015), following the evaporation of HNCO from dust surfaces. Direct surface production of CH_3NCO by radical addiction of CH_3 and OCN has been considered by Cernicharo et al. (2016) and Belloche et al. (2017). Laboratory simulations performed by Ligterink et al. (2018) show that vacuum ultraviolet irradiation of CH_4:HNCO mixtures leads to the formation of CH_3NCO, possibly through the reaction between CH_3 and HNCO. Including this reaction into a gas–grain chemical model, the methyl isocyanate abundances found in IRAS 16293−2422 are reasonably reproduced. Majumdar et al. (2018) present a detailed discussion of the chemistry of CH_3NCO, incorporating updated kinetic data into a gas–grain chemical network. Their simulations indicate that CH_3NCO forms efficiently only on grain surfaces.

In this work, we address the formation of CH_3NCO in the absence of radicals, through reactions involving isocyanic acid and methane in both gas and condensed phases via an advanced computational approach applied, for the first time, to astrochemistry. Traditional computational chemistry provides details that are complementary to laboratory data (Sponer et al. 2016b), including interstellar ice chemistry (Pantaleone et al. 2018; Zamirri et al. 2019). In a previous study, using techniques well suited for structures and energetics of transition states, Majumdar et al. (2018) investigate a suite of reactions leading to the production of CH_3NCO from extremely reactive precursors. Instead, we choose to start from stable reactants to quantitatively estimate the effects carried by solid 'solvents' (ices) in modifying free-energy landscapes and barriers. To this aim, we have employed first-principles molecular dynamics coupled with metadynamics (MetD; Laio & Parrinello 2002; Pietrucci & Saitta 2015), an advanced atomistic simulation technique capable of probing the phase space of complex molecular systems and, at the same time, reconstructing the free-energy landscape of chemical reactions at finite temperature and with exact entropic contributions.

2 METHODS

The formation of methyl isocyanate is here simulated by means of *ab initio* molecular dynamics (AIMD) coupled with MetD. The chemical reaction connecting isocyanic acid and methane with CH_3NCO and molecular hydrogen

$$CH_4 + HNCO \rightarrow CH_3NCO + H_2$$

is thermodynamically characterized in this work at finite temperature (i.e. 200 K) under both gas- and condensed-phase conditions. AIMD simulations were carried out using the software suite CP2K (Hutter et al. 2014) exploiting the Born–Oppenheimer approach (Vande-Vondele et al. 2005) in conjunction with PLUMED-2.3.3 (Tribello et al. 2014), a patch that allows for enhanced sampling calculations. The investigated chemical transformation is reproduced in vacuum starting from isolated, but interacting reactants, in a matrix of pure amorphous water ice, and by placing the HNCO and CH_4 species in a structure of a 50:50 mixture of water and carbon monoxide amorphous ice. Although pieces of evidence indicate that frozen CO is at most 30 per cent of water ice in observed interstellar ices (Boogert, Gerakines & Whittet 2015), the presented investigation is aimed at quantitatively evaluating the effects induced by the presence of specific chemical environments on the free energy of a given reaction rather than exactly reproducing the composition of interstellar ices. Cubic simulation boxes were built for all systems. As for the reproduction of the reaction in vacuum, a cell having side equal to 10.9 Å was adopted, whereas edges of the boxes equal to 15.8 and 16.4 Å were employed for simulations in water, and water and carbon monoxide mixture ices, respectively. Additionally to the reactant species HNCO and CH_4, the water ice sample consisted of 128 H_2O molecules (393 atoms), while the mixture consisted of 56 H_2O and 56 CO species (289 atoms). Albeit seemingly small, these simulation boxes are significantly larger than typical simulation cells employed in astrochemical calculations. Moreover, in our simulations, periodic boundary conditions were applied along all Cartesian directions to mitigate spurious finite-size effects.

By employing AIMD in conjunction with MetD methods, an accurate and direct treatment of finite temperature and entropic contributions is achieved by construction. In fact, all the solvent molecules constituting the environment where the chemical reaction takes place are explicitly treated within the density functional theory (DFT) framework. In particular, a combined plane waves (400 Ry density cut-off) and local TZVP basis set for all atoms is exploited together with Goedecker–Teter–Hutter pseudo-potentials (Goedecker, Teter & Hutter 1996). Exchange and correlation effects are handled by means of the BLYP functional (Becke 1988; Lee, Yang & Parr 1988), along with D3(BJ) dispersion corrections (Grimme et al. 2010; Grimme & Goerigk 2011). In such a way, estimates of the free-energy barriers characterizing the process can be evaluated by including crucial entropic effects (Saitta & Saija 2014; Cassone et al. 2017, 2018a; Pietrucci 2017), which are strongly approximated, if not lacking at all in traditional quantum (astro)chemistry calculations.

The MetD formalism adopted in this work uses the matrices of coordination numbers in order to define a given molecular state, and exploits path Collective Variables (path-CV) MetD (Branduardi, Gervasio & Parrinello 2007; Pietrucci & Saitta 2015) based on two CVs, S and Z, on which the free-energy surface is constructed. S represents the progress along the chemical transformation:

$$s(t) = \frac{\sum_{k=1}^{N_f} k \mathrm{e}^{-\lambda D(\mathbf{R}(t),\mathbf{R}_k)}}{\sum_{k'=1}^{N_f} \mathrm{e}^{-\lambda D(\mathbf{R}(t),\mathbf{R}_{k'})}}, \quad (1)$$

while Z identifies the distance from the predefined (idealized) pathway:

$$z(t) = -\frac{1}{\lambda} \log \left(\sum_{k=1}^{N_f} \mathrm{e}^{-\lambda D(\mathbf{R}(t),\mathbf{R}_k)} \right). \quad (2)$$

Both variables depend on the 'distance', D, between the atomic configuration at a given time and reference structures, as shown for reactants, R, and products, P, in Fig. 1. Formally, as explained in detail in Pietrucci & Saitta (2015), metric of D is defined in the configuration space as

$$D(\mathbf{R}(t), \mathbf{R}_k) = \sum_{IS} \left(C_{IS}(t) - C_{IS}^k \right)^2, \quad (3)$$

where C_{IS} is the coordination number between atom I of species (element) S' and all atoms J of species S, defined by means of a smooth switching function:

$$C_{IS}(t) = \sum_{J \in S} \left[1 - \left(R_{IJ}(t)/R_{SS'}^0 \right)^N \right] / \left[1 - \left(R_{IJ}(t)/R_{SS'}^0 \right)^M \right]. \quad (4)$$

The parameter $R_{SS'}^0$ depends on the two species, since, e.g. a C–H bond is shorter than a C–N bond. We remark that, apart from the latter parameters, the sole input needed to construct the CV are the (trivial) coordination patterns of the reactant and product species, as shown in the ideal matrices of Fig. 1. D hence relies on the coordination patterns of the reactants and products species and

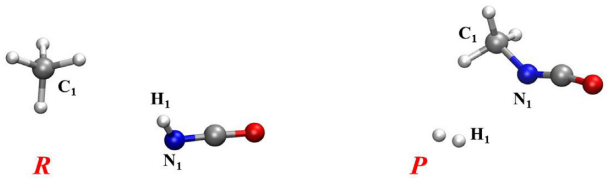

R	O	C	N	H
C_1	0	0	0	4
N_1	0	1	0	1
H_1	0	0	1	0

P	O	C	N	H
C_1	0	0	1	3
N_1	0	2	0	0
H_1	0	0	0	1

Figure 1. Ideal topological coordination matrices defining the reactant, *R*, and product, *P*, states in the gas phase. Matrix elements, indicating the number of first neighbouring atoms of a given species, are shown as integer numbers. During the simulations, they assume decimal values depending on switching functions according to bond lengths. Changes in the local coordination are highlighted by coloured boxes in the matrices. Red, silver, blue, and white colours in the molecular structures refer to oxygen, carbon, nitrogen, and hydrogen atoms, respectively.

this dependence is described through a handful of parameters that enter in the smooth switching functions of equation (4). During the calculation, such parameters have been set to $N = 6$, $M = 12$, and $R^0_{SS'} = 1.8$ Å for $S, S' =$ O, C, N, $R^0_{SS'} = 1.5$ Å for $S =$ O, C, N, $S' =$ H, and $R^0_{SS'} = 1.4$ Å for $S = S' =$ H. Finally, λ is estimated by placing $\lambda \times D(R, P) \sim 2.3$. The MetD potential was composed of Gaussian functions with widths $\sigma_S = 0.02$ and $\sigma_Z = 0.1$, whereas different Gaussian heights equal to 2.4, 4.8, and 7.2 kcal mol^{-1}, deposed every 50 fs (i.e. every 100 MD steps) have been tested. Details of the method development are found in Pietrucci & Saitta (2015), while a recent review on MetD techniques is in Bussi & Laio (2020).

3 RESULTS

The chemistry of interstellar CH_3NCO has been recently reviewed by Majumdar et al. (2018), who also performed detailed electronic-structure calculations based on DFT, exploiting the highly non-local functional M06-2X developed by Zhao & Truhlar (2008). These authors dismiss any gas-phase reaction route leading to the formation of methyl isocyanate. They find that CH_3NCO may be formed efficiently through surface reactions between (i) highly mobile H atoms and H_2CNCO, the end point of a pathway involving the van der Waals complex HCN...CO, and (ii) atomic nitrogen and CH_3CO, formed by the hydrogenation of H_2CCO. The more familiar reaction CH_3 + HNCO has been estimated to have a quite large activation barrier, $\Delta E_b = 8040$ K.

While such conclusions have been conceived for reactions in solid state, calculations have been actually performed in gas phase, as explicitly stated for the process CH_3 + HNCO. Although energy profile diagrams for specific reactions are very well represented, such a description is based on very crude approximations of the entropic contributions of the chemical environment to the free energy. The estimate of the free energy including exact entropic contributions is the scope of this work, in which the ice embedding the reactants is chemically defined at the same level of theory of the reactants themselves (i.e. in explicit solvent).

In the first set of simulations, we have followed the conversion of methane and isocyanic acid into methyl isocyanate and molecular hydrogen under gas-phase conditions. As shown in Fig. 2(a), two (meta)stability basins corresponding to reactants and products are readily identified. Whereas the local minimum of the free-energy surface (FES) associated with the reactants' state occurs at $S \sim 1.15$, the basin ascribed to the products is located around $S \sim 1.85$ (Fig. 2a). Since the topology of the molecular transformation has been here defined as a function of only two states (i.e. reactants and products without the intervention of any intermediate state), the fact that the initial and the final states exhibit values of the CV S close to 1 and 2, respectively, implies a posteriori that the ideal integer coordination numbers shown in the topology matrices of Fig. 1 represent a simplistic yet good approximation for identifying the chemical bonding of the species in gas phase. On top of this, the chemical route connecting the initial and final states is a narrow path (Fig. 2b) possessing a free-energy barrier $\Delta F_b = 141$ kcal mol^{-1} ($\Delta T_b = 70\,450$ K).

The energetic configuration is significantly modified in both quantitative and qualitative ways, once we consider the presence of the ice, either pure water (Fig. 2c) or water mixed with carbon monoxide (Fig. 2e). The free-energy landscape remains topologically simple with the lack of other (meta)stability basins on the FESs. However, the interactions involving the reactants with the local chemical environment are intense enough to sizably modify the ideal integer coordination numbers of the contact matrices via e.g. hydrogen-bond formation. In pure water ices, the (meta)stability basin ascribed to the products falls at $S \sim 1.50$ (Fig. 2c). In H_2O + CO ice mixtures, the locations of FES minima associated with both reactants and products are significantly modified by the presence of a reactive solvent. As shown in Fig. 2(e), the reactant basin falls around $S \sim 1.30$, while that of products is located at $S \sim 1.60$, pointing out how the chemical environment actively modifies the molecular configurations of the host molecules.

In addition, the effect induced by the presence of an active medium, through its own extremely intense local electric field contributions (see e.g. Sellner, Valiev & Kathmann 2013; Laage, Elsaesser & Hynes 2017; Cassone 2020) and partial orbital sharing with the species undergoing chemical transformation, goes well beyond the mere structural modification of the intercalated molecules. In fact, additionally to the fact that the chemical pathways are widened, in particular when carbon monoxide is present (Figs 2e and f), the net effect of the presence of a chemical matrix is a drastic reduction of the free-energy barriers of the conversion of HNCO and CH_4 into H_3CNCO and H_2. In particular, whereas in neat water ice such a reaction is characterized by a $\Delta F_b = 46$ kcal mol^{-1} ($\Delta T_b = 23\,100$), the presence of CO in the ice structure further lowers the free-energy barrier to 35 kcal mol^{-1} ($\Delta T_b = 17\,600$), as shown in Figs 2(d) and (f), respectively. Finally, it is worth noting that according to the Eyring equation (Evans & Polanyi 1935; Eyring 1935), a variation of the free-energy barrier height from 141 kcal mol^{-1} under gas-phase conditions at finite temperature (i.e. 200 K) to a free-energy barrier of 35 kcal mol^{-1} in the presence of a water/carbon monoxide solid matrix at the same temperature is equivalent to an enhancement of e^{106} of the kinetic rate constant of the investigated reaction.

4 CONCLUSIONS

In this work, we have simulated the free-energy variations of the chemical transformation of methane and HNCO to produce methyl isocyanate through state-of-the-art AIMD methods coupled with a MetD approach. We find remarkable differences between reactions taking place in vacuum and those occurring in ices, with the pathways of gas-phase reaction networks practically impassable.

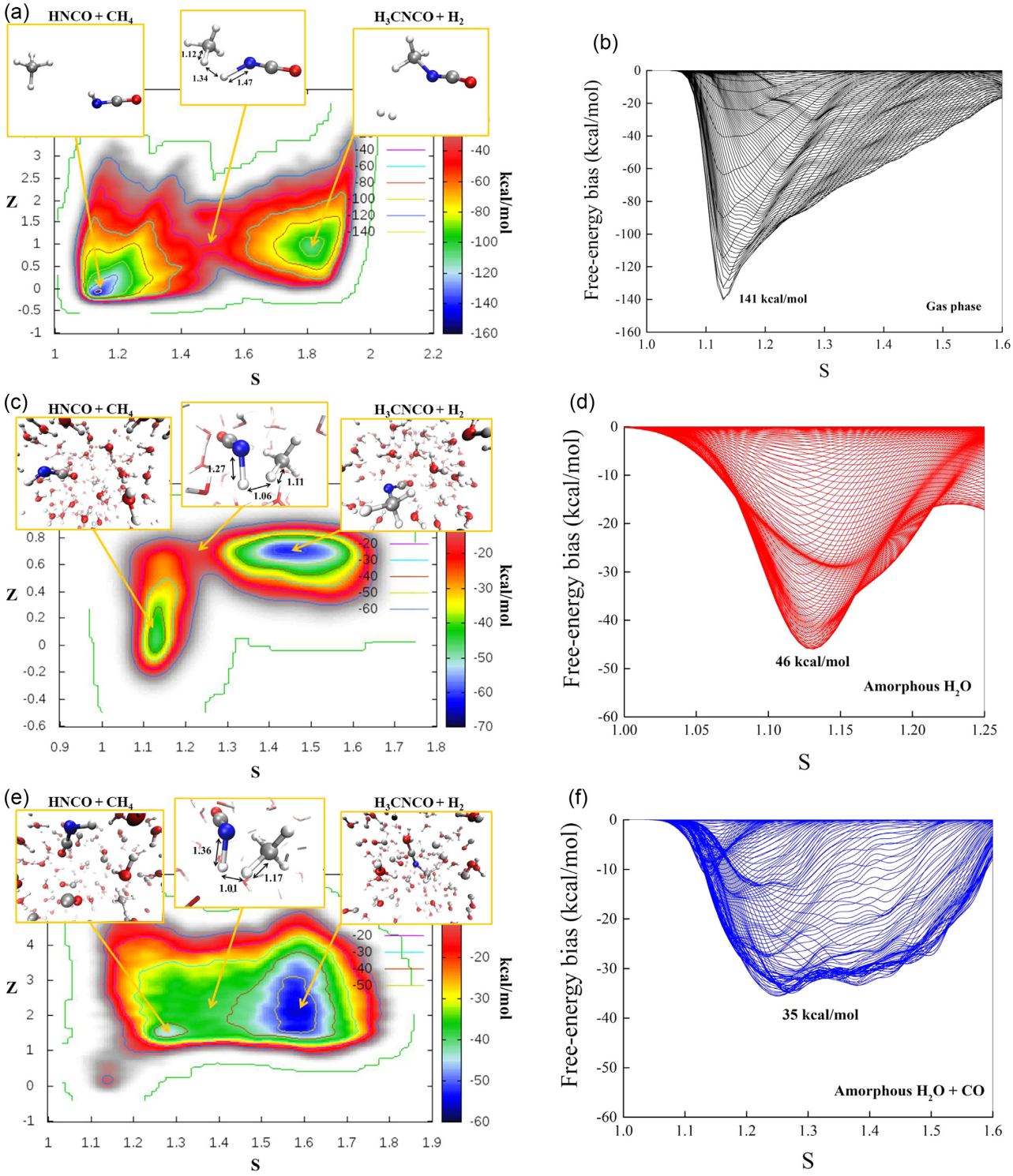

Figure 2. Left-hand panel: Free-energy landscapes of the conversion of methane and isocyanic acid into methyl isocyanate and molecular hydrogen in gas phase (a), in amorphous water ice (c), and in a 50:50 H_2O:CO ice (e). Right-hand panel: Time development of the free-energy biases necessary to the reactants for escaping from their own free-energy local minimum in gas phase (b), in amorphous water ice (d), and in a 50:50 H_2O:CO ice (f). The bias corresponds to the negative of the free-energy barrier separating reactant and product states, the latter being shown in the insets of the free-energy landscapes along with a representative, approximated, transition state structure and relevant interatomic distances in Å (left-hand panel).

The resulting energy barriers in ices are, however, still too high to allow for a straightforward conversion of methane and HNCO into CH_3NCO, even in warm interstellar regions. Some additional mechanisms would be required, such as grain–grain collisions arising from magnetohydrodynamic turbulence (e.g. Yan, Lazarian & Draine 2004). While high-velocity impacts may have interesting chemical consequences (Cassone et al. 2018b), low-velocity collisions can lead to grain heating (e.g. d'Hendecourt et al. 1982) and ice sublimation.

According to the description presented by Yan et al. (2004), turbulent acceleration is more effective for large grains than for small grains, enhancing the rate of grain–grain collisions. In cold regions, for reasonable strengths of magnetic fields, the relative velocities gained by submicron-sized grains may be $\gtrsim 1$ km s^{-1} (Yan et al. 2004). This translates to Hugoniot temperatures of ∼1000–2000 K (Goldman et al. 2010), providing a sharp increase of the exponential cut-off in the Eyring equation of more than 30 orders of magnitude. Albeit such a temperature increase would certainly lead to ice sublimation, the chemistry triggered by these kinds of impacts occurs at timescales predating those of all mechanical processes. In fact, the first chemical effects are generally observed about 100 fs after the impact (Cassone et al. 2018b), while sublimation is expected to occur at least one order of magnitude later. During that temporal window, the effects induced by the solvent, stemming from both the compressed and not directly compressed portions, on the reactants are even more effective due to compression. This way, the catalytic effects carried by the solvent via quantum chemistry processes and local intense electric fields are sensibly present even in impact events leading to a significant increase of the local temperature and hence to phase transitions. Thus, in specific situations the reaction under investigation may become competitive with other proposals put forward in the literature.

Albeit it is commonly accepted that many characteristics of the gas-phase reaction dynamics persist under condensed-phase conditions, additional complexities associated with the presence of the solvent are open to investigation (Orr-Ewing 2015). This way, beyond local solutions to particular problems, the critical point raised in this work is the definition – on quantum and thermodynamical bases – of the role played by the solvent, whose presence reduces dramatically the free-energy barriers. Such a finding is perfectly in line with important pieces of evidence emerged from quantum chemical investigations (see e.g. Rimola et al. 2005; Pantaleone et al. 2018; Zamirri et al. 2019). Thus, ices not only may act as gatherers of reactants, but may also create favourable thermodynamic conditions for chemical evolution. Finally, the powerful computational methods presented in this work, by exactly treating crucial entropic contributions typically crudely approximated (or lacking) in traditional astrochemical calculations, offer the opportunity to globally explore chemical reactions occurring in the interstellar medium, and discriminate among competitive reaction channels.

DATA AVAILABILITY

The data underlying this article will be shared on request to the corresponding authors.

REFERENCES

Altwegg K. et al., 2017, MNRAS, 469, S130
Becke A. D., 1988, Phys. Rev. A, 38, 3098
Belloche A. et al., 2017, A&A, 601, A49
Bonfio C., Russell D. A., Green N. J., Mariani A., Sutherland J. D., 2020, Chem. Sci., 11, 10688
Boogert A. C. A., Gerakines P. A., Whittet D. C. B., 2015, ARA&A, 53, 541
Branduardi D., Gervasio F. L., Parrinello M., 2007, J. Chem. Phys., 126, 54103
Bussi G., Laio A., 2020, Nat. Rev. Phys., 2, 200
Carney M. T., Hogerheijde M. R., Loomis R. A., Salinas V. N., Öberg K. I., Qi C., Wilner D. J., 2017, A&A, 605, A21
Cassone G., 2020, J. Phys. Chem. Lett., 11, 8983
Cassone G., Pietrucci F., Saija F., Guyot F., Saitta A. M., 2017, Chem. Sci., 8, 2329
Cassone G., Sponer J., Sponer J. E., Pietrucci F., Saitta A. M., Saija F., 2018a, Chem. Commun., 54, 3211
Cassone G. et al., 2018b, ApJ, 866, L23
Cernicharo J. et al., 2016, A&A, 587, L4
Cheung A. C., Rank D. M., Townes C. H., Thornton D. D., Welch W. J., 1968, Phys. Rev. Lett., 21, 1701
d'Hendecourt L. B., Allamandola L. J., Baas F., Greenberg J. M., 1982, A&A, 109, L12
Evans M. G., Polanyi M., 1935, Trans. Faraday Soc., 31, 875
Eyring H., 1935, J. Chem. Phys., 3, 107
Favre C. et al., 2018, ApJ, 862, L2
Ferus M., Nesvorny D., Šponer J., Kubelik P., Michalčíková R., Shestivská V., Šponer J. E., Civiš S., 2015, Proc. Natl. Acad. Sci. USA, 112, 657
Goedecker S., Teter M., Hutter J., 1996, Phys. Rev. B, 54, 1703
Goesmann F. et al., 2015, Science, 349, aab0689
Goldman N., Reed E. J., Fried L. E., Kuo I.-F. W., Maiti A., 2010, Nat. Chem., 2, 949
Gorai P., Bhat B., Sil M., Mondal S. K., Ghosh R., Chakrabarti S. K., Das A., 2020, ApJ, 895, 88
Grimme S., Goerigk L., 2011, J. Comput. Chem., 32, 1456
Grimme S., Antony J., Ehrlich S., Krieg H., 2010, J. Chem. Phys., 132, 154104
Halfen D. T., Ilyushin V. V., Ziurys L. M., 2015, ApJ, 812, L5
Hutter J., Iannuzzi M., Schiffmann F., VandeVondele J., 2014, Wiley Interdiscip. Rev. Comput. Mol. Sci., 4, 15
Laage D., Elsaesser T., Hynes J. T., 2017, Struc. Dyn., 4, 044018
Laio A., Parrinello M., 2002, Proc. Natl. Acad. Sci. USA, 99, 12562
Lee C., Yang W., Parr R. G., 1988, Phys. Rev. B, 37, 785
Ligterink N. F. W. et al., 2017, MNRAS, 469, 2219
McGuire B. A., 2018, ApJS, 239, 17
Majumdar L., Loison J.-C., Ruaud M., Gratier P., Wakelam V., Coutens A., 2018, MNRAS, 473, L9
Marcelino N., Agúndez M., Cernicharo J., Roueff E., Tafalla M., 2018, A&A, 612, L10
Martín-Doménech R., Rivilla V. M., Jiménez-Serra I., Quénard D., Testi L., Martín-Pintado J., 2017, MNRAS, 469, 2230
Öberg K.I., Guzmán V.V., Furuya K., Qi C., Aikawa Y. A., Sean M., Loomis R., Wilner D. J., 2015, Nature, 520, 198
Orr-Ewing A. J., 2015, Annu. Rev. Phys. Chem., 66, 119
Pantaleone S., Ugliengo P., Sodupe M., Rimola A., 2018, Chem. Eur. J., 24, 1629
Pascal R., Boiteau L., Commeyras A., 2005, From the Prebiotic Synthesis of α −Amino Acids Towards a Primitive Translation Apparatus for the Synthesis of Peptides. Springer, Berlin, p. 69
Pietrucci F., 2017, Rev. Phys., 2, 32
Pietrucci F., Saitta A. M., 2015, Proc. Natl. Acad. Sci. USA, 112, 15030
Podio L. et al., 2019, A&A, 623, L6
Rimola A., Tosoni S., Sodupe M., Ugliengo P., 2005, Chem. Phys. Lett., 408, 295
Rubin R. H., Swenson G. W. J., Benson R. C., Tigelaar H. L., Flygare W. H., 1971, ApJ, 169, L39
Saitta A. M., Saija F., 2014, Proc. Natl. Acad. Sci. USA, 111, 13768
Saladino R., Carota E., Botta G., Kapralov M., Timoshenko G. N., Rozanov A. Y., Krasavin E., Di Mauro E., 2015, Proc. Natl. Acad. Sci. USA, 112, E2746
Sellner B., Valiev M., Kathmann S. H., 2013, J. Phys. Chem. B, 117, 10869
Snyder L. E., Buhl D., 1972, ApJ, 177, 619
Sponer J. E., Mladek A., Sponer J., Fuentes-Cabrera M., 2012, J. Phys. Chem. A, 116, 720
Sponer J. E. et al., 2016a, Chem. Eur. J., 22, 3572
Sponer J. E. et al., 2016b, Phys. Chem. Chem. Phys., 18, 20047

Suárez-Marina I., Abul-Haija Y. M., Turk-MacLeod R., Gromski P. S., Cooper G. J. T., Olive A. O., Colon-Santos S., Cronin L., 2019, Commun. Chem., 2, 28
Tribello G. A., Bonomi M., Branduardi D., Camilloni C., Bussi G., 2014, Comput. Phys. Commun., 185, 604
VandeVondele J., Krack M., Mohamed F., Parrinello M., Chassaing T., Hutter J., 2005, Comput. Phys. Commun., 167, 103
Walsch C. et al., 2016, ApJ, 823, L10
Yan H. R., Lazarian A., Draine B. T., 2004, ApJ, 616, 895
Zamirri L., Ugliengo P., Ceccarelli C., Rimola A., 2019, ACS Earth Space Chem., 3, 8, 1499
Zhao Y., Truhlar D. G., 2008, Theor. Chem. Acc., 120, 215

This paper has been typeset from a TEX/LATEX file prepared by the author.